

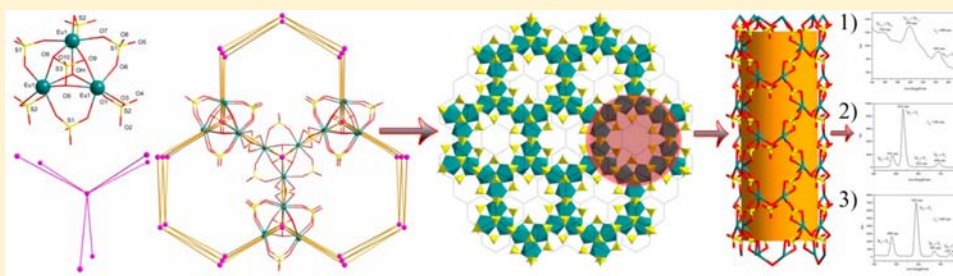
$(C_4N_2H_{12})_3[Ln_3(OH)(SO_4)_7]$ (Ln = Sm, Eu, and Tb): A Series of Honeycomb-like Open-Framework Lanthanide Sulfates with Extra-Large Channels Containing 24-Membered Rings

Deng Zhang,[†] Yun Lu,[†] Dunru Zhu,[†] and Yan Xu^{*,†,‡}

[†]State Key Laboratory of Materials-oriented Chemical Engineering, Nanjing University of Technology, Nanjing 210009, People's Republic of China

[‡]State Key Laboratory of Coordination Chemistry, Nanjing University, Nanjing 210093, People's Republic of China

S Supporting Information



ABSTRACT: Three novel organic amine templated honeycomb-like lanthanide sulfates, $(C_4N_2H_{12})_3[Ln_3(OH)(SO_4)_7]$ (Ln = Sm (1), Eu (2), and Tb (3)), with extra-large channels containing 24-membered rings (24MR) have been synthesized by using chair form piperazine as the structure-directing agent under one-pot solvothermal reactions. The three compounds are isostructural, and the open framework of the title compounds is the first lanthanide sulfate example with extra-large channels containing 24MR. It has an *acs* framework topology. The three compounds are strong luminescent materials that display characteristic Sm^{3+} , Eu^{3+} , and Tb^{3+} emission bands in the visible region. The observed second-harmonic generation efficiencies of the three compounds are all 0.4 times that of urea. TGA profiles and XRD measurements demonstrate their high thermal stability.

INTRODUCTION

Great efforts have been made to synthesize new porous materials with different structural characteristics or compositions, while the topological microporous structures with extra-large-pore (more than 12-membered ring channels) open frameworks are extremely significant because of the widespread applications of these porous materials in catalysis and the separation of large molecules, such as pharmaceuticals and heavy oils. Since the preparation of VPI-5, the first molecular sieve aluminophosphate containing extra-large 18-membered rings (18MR),¹ some open frameworks, including metal phosphates, aluminosilicates, and germanates with extra-large pores, such as UTD-1 (14MR),^{2a,b} CIT-5 (14MR),^{2c} $AlPO_4-8$ (14MR),^{2d} Cloverite (20MR),^{3a} JDF-20 (20MR),^{3b} $[Zn_3(O_3PCH_2COO)_2(O_3PCH_2COOH)][(NH_3CH_2CH_2NH_3)-(btc)]$,^{4a} ND-1 (24MR),^{4b} NTHU1 (24MR),^{4c} FD4 (24MR),^{4d} VSB-1, VSB-5 (24MR),^{4e,f} ASU-16 (24MR),^{4g} FJ-1 (24MR),^{4h} ZnHPO-CJ1 (24MR),⁴ⁱ and SU-M (30MR),⁵ have been discovered. Recently, one of the important advances in solid-state chemistry has been the study of lanthanide sulfates.^{6–11} Compared with Al, Ge, and 3d transition metals, the rare-earth elements can adopt flexible coordination numbers from 8 (LnO_8) to 12 (LnO_{12}) and longer Ln–O bond lengths. The

high coordination number offers the possibility to make open frameworks with high charge densities, which may result in novel topological frameworks with extra-large pores.^{4d} Unfortunately, to date, only $(C_2H_8N)_9[Ln_5(SO_4)_{12}] \cdot 2H_2O$ (Ln = La, Ce, Sm, Eu, Tb) with 20MR pores were prepared by using a small template (dimethylamine).¹¹ When large organic amines were chosen as templates, Ln^{3+} was easily coordinated by water to prevent further connection, and isolated Ln–O–S clusters, 1D chains, and 2D layered lanthanide sulfates were obtained.¹⁰ Solvent plays an important role for an attempted synthesis, as the solvent might interact with the organic amines and facilitate the interactions between the organic amines and the framework.¹² Herein, we used a mixture of water and glycol as solvent and piperazine as the template to successfully synthesize three novel organic amine templated honeycomb-like lanthanide sulfates, $(C_4N_2H_{12})_3[Ln_3(OH)(SO_4)_7]$ (Ln = Sm (1), Eu (2), and Tb (3)) with extra-large channels containing 24MR. The framework of all three compounds presents an *acs* net topology ($4^9 \cdot 6^6$), which was assigned as the default net for the assembly of trigonal prismatic building

Received: December 17, 2012

Published: March 6, 2013

Table 1. Crystal Data and Structure Refinement for 1–3

	Sm(1)	Eu(2)	Tb(3)
empirical formula	C ₁₂ H ₃₇ N ₆ O ₂₉ S ₇ Sm ₃	C ₁₂ H ₃₇ N ₆ O ₂₉ S ₇ Eu ₃	C ₁₂ H ₃₇ N ₆ O ₂₉ S ₇ Tb ₃
formula weight	1404.95	1409.78	1430.66
temperature (K)	296(2)	296(2)	296(2)
wavelength (Å)	0.71073	0.71073	0.71073
crystal system	trigonal	trigonal	trigonal
space group	P31c	P31c	P31c
unit cell dimensions	<i>a</i> = 14.3551(8) Å <i>b</i> = 14.3551(8) Å <i>c</i> = 10.1132(11) Å α = 90° β = 90° γ = 120°	<i>a</i> = 14.3280(9) Å <i>b</i> = 14.3280(9) Å <i>c</i> = 10.0966(7) Å α = 90° β = 90° γ = 120°	<i>a</i> = 14.2698(16) Å <i>b</i> = 14.2698(16) Å <i>c</i> = 10.066(2) Å α = 90° β = 90° γ = 120°
volume (Å ³)	1804.8(2)	1795.1(2)	1775.1(5)
Z	2	2	2
<i>D_c</i> (Mg/m ³)	2.585	2.608	2.677
μ (mm ⁻¹)	5.335	5.698	6.439
<i>F</i> (000)	1362	1368	1380
θ range (deg)	1.64–26.00	1.64–25.98	1.65–25.98
limiting indices	−17 ≤ <i>h</i> ≤ 15 −17 ≤ <i>k</i> ≤ 17 −12 ≤ <i>l</i> ≤ 12	−17 ≤ <i>h</i> ≤ 17 −17 ≤ <i>k</i> ≤ 17 −10 ≤ <i>l</i> ≤ 12	−17 ≤ <i>h</i> ≤ 17 −17 ≤ <i>k</i> ≤ 17 −12 ≤ <i>l</i> ≤ 11
reflns collected	13 024	9922	12 774
indep reflns	2365	2179	2291
<i>R</i> (int)	0.0684	0.0335	0.0625
completeness to θ	99.8%	99.7%	99.8%
data/restraints/params	2365/1/169	2179/1/172	2291/1/173
GOF	1.016	1.044	1.077
<i>R</i> 1 ^a , <i>wR</i> 2 ^b [<i>I</i> > 2 σ (<i>I</i>)]	0.0305, 0.0581	0.0197, 0.0453	0.0291, 0.0603
<i>R</i> 1, <i>wR</i> 2 (all data)	0.0351, 0.0597	0.0201, 0.0454	0.0324, 0.0653

$$^a R1 = \sum ||F_o| - |F_c|| / \sum |F_o|. \quad ^b wR2 = \sum [w(F_o^2 - F_c^2)^2] / \sum [w(F_o^2)^2]^{1/2}.$$

blocks.^{14a} The nonlinear optical properties and luminescence properties of the three compounds have also been investigated in detail.

EXPERIMENTAL SECTION

Materials and Physical Measurements. All chemicals were purchased from commercial sources and used without further purification. Powder X-ray diffraction (PXRD) was obtained on a Bruker D8X diffractometer equipped with monochromatized Cu *K* α (λ = 1.5418 Å) radiation at room temperature. Data were collected in the range of 5–50°, and the experimental XRD patterns are in agreement with the patterns simulated on the basis of the single-crystal structures (Figures S4–S6, Supporting Information). The element analyses were performed on a PerkinElmer 2400 element analyzer. The infrared (IR) spectrum was recorded within the 400–4000 cm⁻¹ region on a Nicolet Impact 410 FTIR spectrometer using KBr pellets. A NETZSCH STA 449C unit was applied to carry out the TG analyses under a nitrogen atmosphere from 25 to 1100 °C at a heating rate of 10 °C/min. Solid-state luminescence properties were carried out at an F-4600 FL spectrophotometer.

General Procedures. A mixture of Ln₂O₃ (0.2000 g) and piperazine (0.2000 g) was added into 5.0 mL of a mixed solvent of glycol (3.0 mL) and H₂O (2.0 mL); then 3.0 mmol of concentrated H₂SO₄ (98 wt %) was added to the mixture. The resulting mixture was then vigorously stirred for an hour and was introduced into a 25 mL Teflon-lined stainless steel autoclave. The autoclave was sealed and heated at 453 K for 6 days. After cooling to room temperature, the product was washed with ethanol, and colorless block crystals were obtained. For compound 1: Yield: 0.0218 g, 40.2% based on Sm. Anal. Calcd for C₁₂H₃₇N₆O₂₉S₇Sm₃ (1404.95): C, 10.26; H, 2.65; N, 5.98. Found: C, 10.21; H, 2.70; N, 5.88. IR spectrum (cm⁻¹, KBr pellet): 3421 (s), 1605 (s), 1468 (w), 1395 (m), 1118 (vs), 1075 (s), 663 (m),

610 (s). For compound 2: Yield: 0.0241 g, 45.2% based on Eu. Anal. Calcd for C₁₂H₃₇N₆O₂₉S₇Eu₃ (1409.78): C, 10.22; H, 2.65; N, 5.96. Found: C, 10.17; H, 2.81; N, 5.91. IR spectrum (cm⁻¹, KBr pellet): 3444 (vs), 1608 (s), 1469 (w), 1390 (m), 1308 (w), 1120 (vs), 1082 (s), 660 (m), 613 (s). For compound 3: Yield: 0.0219 g, 42.2% based on Tb. Anal. Calcd for C₁₂H₃₇N₆O₂₉S₇Tb₃ (1430.66): C, 10.07; H, 2.61; N, 5.87. Found: C, 9.98; H, 2.74; N, 5.79. IR spectrum (cm⁻¹, KBr pellet): 3425 (s), 1605 (s), 1396 (w), 1304 (m), 1115 (vs), 1081 (s), 660 (m), 610 (s).

X-ray Crystallography. Data for the compounds of 1–3 were collected by using a Bruker Apex 2 CCD single-crystal diffractometer with Mo *K* α radiation (λ = 0.71073 Å) at 298 K using the ω -2 θ scan method. The single crystals of all compounds 1–3 were chosen onto a thin glass fiber by epoxy glue in air for data collection. The SHELX software package (Bruker) was used to solve and refine the structures. Absorption corrections were applied empirically using the SADABS program. All the non-hydrogen atoms were refined anisotropically. The hydrogen atoms of organic molecules were placed in calculated positions, assigned isotropic thermal parameters, and allowed to ride on their parent atoms, while the proton of the hydroxyl group was not located. All calculations were performed using the SHELX97 program package.¹⁸ Further details of the X-ray structural analyses for compounds 1–3 are given in Table 1, and selected bond lengths and angles are listed in Tables S1 and S2 (Supporting Information).

RESULTS AND DISCUSSION

Synthesis. Hydrothermal synthesis has recently been demonstrated to be a powerful method in the synthesis of solid-state lanthanide sulfates. During a specific hydrothermal synthesis, many factors can affect the nucleation and crystal growth of the final products, such as the type of initial reactants,

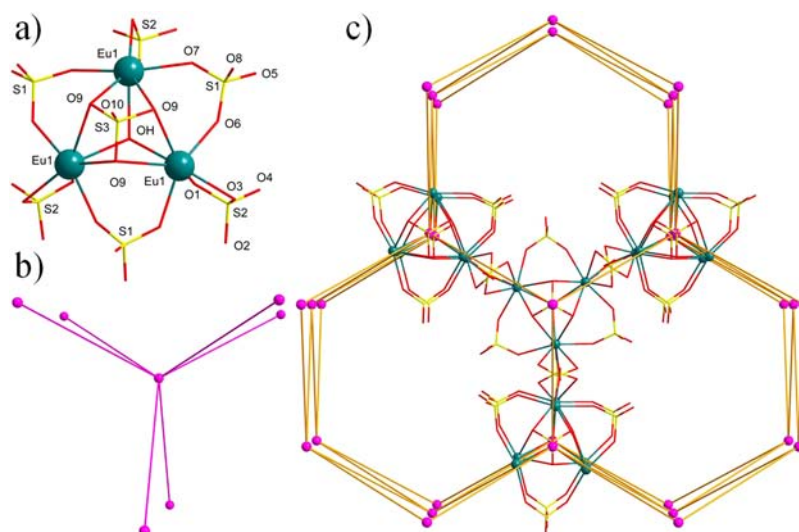


Figure 1. (a) The $[\text{Eu}^{\text{III}}_3(\text{OH})(\text{SO}_4)_7]$ cluster as an SBU. (b) A reduced graph of a central 6-connected node surrounded by six nodes. (c) A ball-and-stick diagram to show a central 6-connected SBU surrounded by six SBUs, where the pink balls stand for the 6-connected nodes and the yellow sticks correspond to the connectivity between the nodes.

starting concentrations of the reactants, pH values, solvents, reaction temperature, and time. In this work, solvents (a mixture of glycol and water) play an important role in the formation of $(\text{C}_4\text{N}_2\text{H}_{12})_3[\text{Ln}_3(\text{OH})(\text{SO}_4)_7]$ ($\text{Ln} = \text{Sm}, \text{Eu},$ and Tb), as the solvent might interact with the organic amines and facilitate the interactions between the organic amines and the framework.¹² If we change the solvent into a mixture of ethanol and water, we got a different 3D $\text{La}_2(\text{H}_2\text{O})_2(\text{C}_4\text{H}_{12}\text{N}_2)(\text{SO}_4)_4$.^{8a}

Crystal Structure. The three compounds are isostructural, and the open framework is the first porous lanthanide sulfate with extra-large channels containing 24MR. It has an *acs* framework topology ($4^9\cdot 6^6$) with the space group $P31c$ (No. 159, standard setting). Single-crystal structural analyses reveal that $(\text{C}_4\text{N}_2\text{H}_{12})_3[\text{Ln}_3(\text{OH})(\text{SO}_4)_7]$ ($\text{Ln} = \text{Sm}$ (1), Eu (2), and Tb (3)) is constructed from a macroanionic $[\text{Ln}_3(\text{OH})(\text{SO}_4)_7]_n^{6n-}$ framework and piperazine counterions. Take compound 2 as an example. The asymmetric unit contains 21 non-hydrogen atoms, 15 of which belong to the open framework, including one europium atom, one oxygen from the hydroxyl, and three SO_4^{2-} groups. $\text{Eu}(1)$ is coordinated by nine oxygen atoms; the bond distances of $\text{Eu}-\text{O}$ vary from 2.343(2) to 2.657(2) Å, while the angles $\text{O}-\text{Eu}-\text{O}$ are between 55.24(9) and 145.86(8)°, which are comparable with other reported Eu compounds.^{9,10c,11a,b} Three crystallographically independent S atoms can be divided into three groups: $\text{S}(1)$ are bonded by two $\mu_2\text{-O}$ and two O_t (terminal O atoms) to make 2 $\text{S}-\text{O}-\text{Eu}$ linkages, $\text{S}(2)$ are bonded by four $\mu_2\text{-O}$ atoms to make 4 $\text{S}-\text{O}-\text{Eu}$ linkages, and $\text{S}(3)$ is coordinated by three $\mu_3\text{-O}$ and one O_t to make three $\text{S}-\text{O}-\text{Eu}$ linkages. Three $[\text{S}(1)\text{O}_4]$ groups, three $[\text{S}(2)\text{O}_4]$ groups, one $[\text{S}(3)\text{O}_4]$ group, and a hydroxyl group bridged three europium ions by six $\mu_2\text{-O}$ and four $\mu_3\text{-O}$ to form a $[\text{Eu}^{\text{III}}_3(\text{OH})(\text{SO}_4)_7]$ secondary building unit (SBU) (Figure 1a). The topological trigonal prismatic 6-connected $[\text{Eu}^{\text{III}}_3(\text{OH})(\text{SO}_4)_7]$ SBUs are then interconnected via the sulfate groups to form a network of a uninodal *acs* net topology (Figure 1b). Although the *acs* net topology ($4^9\cdot 6^6$) is a semiregular net, a few examples present an *acs* net topology with trigonal prismatic 6-connected nodes^{13–16} (Figure 1c). To the best of our knowledge, the

acs topological open framework has not been found in lanthanide sulfates.

Figure 2a shows a 24MR formed by the connection of six SBUs. Six protonated piperazine cations reside in the 24MR

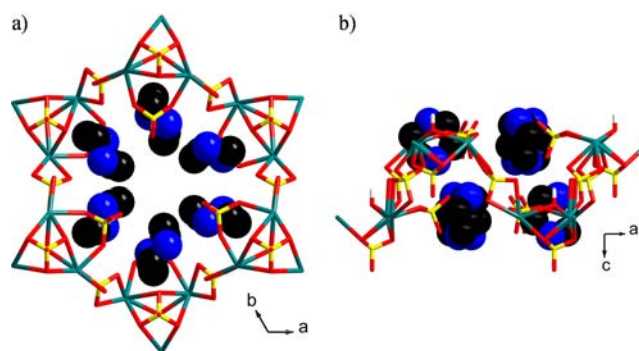


Figure 2. Structure of the 24-membered ring in 2 constructed from 6 SBUs viewing along the c axis (a) and the b axis (b).

and form strong hydrogen-bonding interactions between the N atom of organic amine and O atoms of the framework (Figure S1, Supporting Information); if we take compound 1, for example, the $\text{N}\cdots\text{O}$ distances are between 2.751(5) and 3.340(4) Å. Hydrogen bonds for the three compounds are given in Table S3 (Supporting Information). The central part of the 24MR is hollow, and protonated piperazine cations are found near the inorganic framework. Interestingly, these SBUs are not in a plane, but with a zigzag fashion, to appear as a zigzag 24MR extending along the crystallographic b axis (Figure 2b). Because of the strong hydrogen-bonding and static interactions, the 3D open framework is not stable after removing protonated piperazine cations.

The structure of the three compounds has similarity with the mesoporous SBA-15 materials, both composed of channels in hexagonal honeycomb arrays.¹⁷ The improvement is that we can get the structure on an atomic level compared with SBA-15. Figure 3a shows the polyhedral view of projection of channels containing 24MR running along the crystallographic c axis and leading to a 3D honeycomb array. Each channel containing

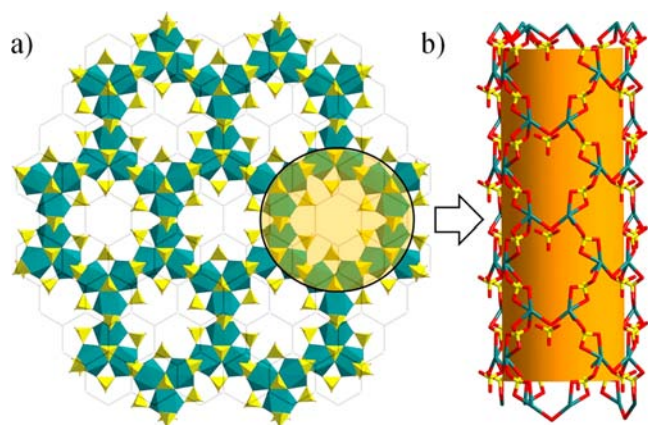
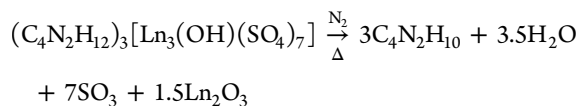


Figure 3. (a) Polyhedral view of the projection of the 24-membered channels running along the crystallographic *c* axis and leading to a 3D honeycomb array. (b) One 24-ring tube with 12-ring side pockets.

24MR is tubular, and the walls are constructed of 12MR side pockets, while adjacent channels containing 24MR are orderly arranged in closed packing just like the mesoporous materials (SBA-15). Each of the channels containing 24MR is surrounded by six 24-membered channels, and they are connected by sharing the SBUs. Strikingly, each of the SBUs is sharing by three channels. Due to their SBA-15-like close packing, its framework density, 11.08 polyhedral per 1000 Å³, is somewhat similar to the values for ND-1(12.1),^{4b} NTHU-1(11.9),^{4c} FDU-4(11.1),^{4d} and ZnHPO-CJ1(11.6).⁴ⁱ

IR Spectra. Extended solids of 1–3 have similar FT-IR spectra showing only slight shifts in some band positions (Figures S8–S10, Supporting Information). We take 2 as an example. Because the local symmetry around the sulfate anion decreases as a consequence of coordination to the Ln(III) ion, the S–O stretching vibrations are split to the bands 1120 and 1082 cm⁻¹, while O–S–O bending vibrations are split to the bands 613 and 605 cm⁻¹, as shown in Figure S9 (Supporting Information). The stretching and bending vibrations of the C–H, C–N, and N–H bonds appear in the regions between 1608 and 1308 cm⁻¹. The band at 660 cm⁻¹ is attributed to the stretching vibrations of the Eu–O bond.

PXRD Patterns and Thermal Properties. The experimental PXRD patterns of the three compounds obtained at room temperature are shown in Figures S4–S6 (Supporting Information). Their main peak positions keep up a correspondence with each other, indicating the phase purity of the samples. The reflection intensity difference between the experimental and simulated patterns could be caused by the variation in the preferred orientation of powder samples during the PXRD data collection. TGA experiments were conducted to determine the thermal stability of the isomorphous 1–3 under a nitrogen atmosphere from 25 to 1100 °C. Thermogravimetric analysis shows that the three compounds have a similar weight loss curve. We take compound 1 as an example; the total weight loss of 1 is 60.3%, which is in agreement with the calculated value (62.8%)



As shown in Figure 4, the weight loss of 22.3% in the range of 50–450 °C corresponds to the removal of the organic amine

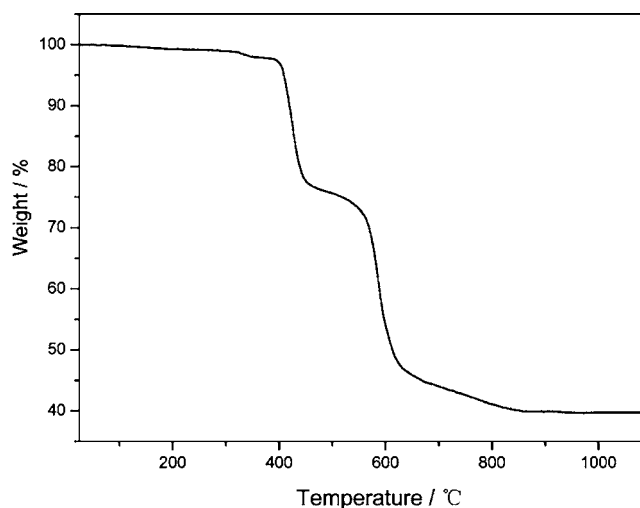


Figure 4. TG curve of 1 (temperature variation from 25 to 1000 °C at a heating rate of 10 °C·min⁻¹ in a N₂ atmosphere).

and water (the calculated value is 22.9%). While the weight loss of 38.0% in the range of 450–1100 °C can be attributed to the loss of SO₃ (the calculated value is 39.9%), the final product is Sm₂O₃.¹¹ We also take compound 3 heated at 350 °C in a muffle furnace for 24 h, and perform PXRD analysis. Their main peak positions still correspond with each other, as shown in Figure S7 (Supporting Information). Therefore, we know that the samples are stable up to 350 °C and the framework is also retained. Such a high decomposition temperature of the piperazine group is not surprising, due to the fact that the piperazine group is occluded in the cavities and involves a strong hydrogen bond to the framework (Figure S1, Supporting Information). Such a high thermal stability has also been observed for the other reported lanthanum piperazine sulfate.¹⁹

Nonlinear Optical Measurement. Second-order nonlinear optical effects for the powder samples of (C₄N₂H₁₂)₃[Ln₃(OH)(SO₄)₇] (Ln = Sm (1), Eu (2), and Tb (3)) were investigated by optical second-harmonic generation (SHG) at room temperature. SHG intensity data were obtained by placing the powder sample in an intense fundamental beam from a Q-switched Nd:YAG laser with a wavelength 1064 nm. The output (λ = 532 nm) was filtered first to remove the multiplier and then displayed on an oscilloscope. This procedure was repeated using a standard NLO material (microcrystalline urea), and the ratio of the second-harmonic intensity outputs was calculated. We observed an SHG efficiency of 0.4 times that of urea for all three compounds (C₄N₂H₁₂)₃[Ln₃(OH)(SO₄)₇] (Ln = Sm (1), Eu (2), and Tb (3)).

Photoluminescence Property. Luminescent properties of the three compounds were also investigated. The emission spectra of the three complexes were measured in the solid state at room temperature. As shown in Figure 5a, the emission spectrum of compound 1 exhibits the characteristic transition of the Sm³⁺ ion attributed to ⁴G_{5/2} → ⁶H_J (J = 5/2, 7/2, 9/2) transitions, whereas the emission spectrum of compound 2 exhibits the characteristic transition of the Eu³⁺ ion attributed to ⁵D₀ → ⁷F_J (J = 0, 1, 3, 4) transitions (Figure 5b). Compound 3 shows green luminescence, as shown in Figure 5c; the emission spectrum exhibits the characteristic transition of the Tb³⁺ ion attributed to ⁵D₄ → ⁷F_J (J = 6, 5, 4, 3) transitions. The luminescence intensities of compounds 2 and 3 are much

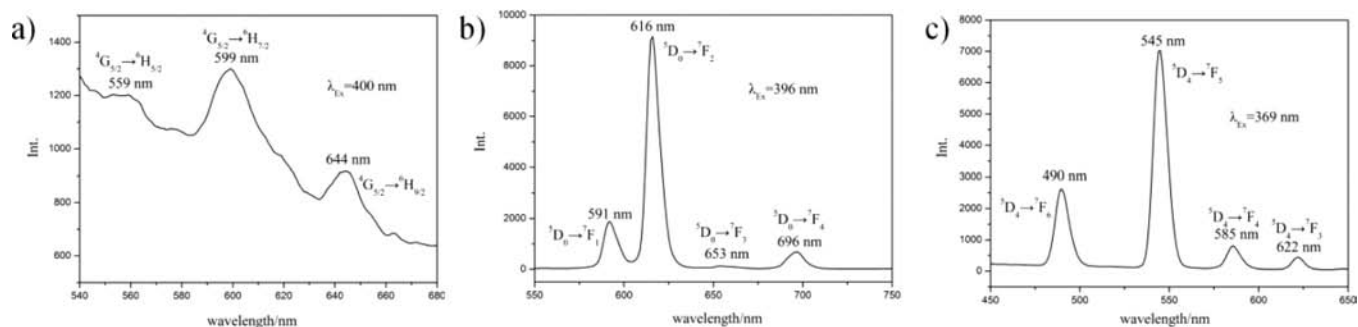


Figure 5. (a) The solid-state photoluminescence spectrum of compound **1**. The excitation wavelength is 400 nm, and spectra are taken at room temperature. (b) The solid-state photoluminescence spectrum of compound **2**. The excitation wavelength is 396 nm, and spectra are taken at room temperature. (c) The solid-state photoluminescence spectrum of compound **3**. The excitation wavelength is 369 nm, and spectra are taken at room temperature.

stronger than the reported Eu (Tb) sulfates reported previously.¹¹ The enhanced fluorescence efficiency of **2** and **3** is attributed to the fact that the SBA-15-like closed-packing environment increases the rigidity of Eu (Tb) atoms effectively and reduces the loss of energy by vibrations. The very strong luminescence in the green and red light regions indicates that **2** and **3** are excellent candidates for green and red fluorescent materials, respectively.

CONCLUSIONS

To the best of our knowledge, these three compounds are the first lanthanide sulfates with extra-large channels containing 24MR since $(C_2H_8N)_9[Eu_5(SO_4)_{12}] \cdot 2H_2O$ with pores containing 20MR was found. They provide important information of the configuration of extra-large pores. They are also important examples of an inorganic open framework of an *acs* net topology with trigonal prismatic 6-connected nodes and completely inorganic linkers. The formation of these three compounds indicates that organic amine together with the solvothermal condition may control the framework of 3D rare earth sulfates with large pores. The present work has great significance both for rare-earth chemistry and porous materials science.

ASSOCIATED CONTENT

Supporting Information

X-ray crystallographic data in CIF format, IR spectra, and TGA. This material is available free of charge via the Internet at <http://pubs.acs.org>.

AUTHOR INFORMATION

Corresponding Author

*E-mail: yanxu@njut.edu.cn. Tel: 86-25-83587857. Fax: 86-25-83211563.

Notes

The authors declare no competing financial interest.

ACKNOWLEDGMENTS

This work was supported by the National Natural Science Foundation of China (Grants 20971068 and 21171093) and Jiangsu Province (Grant BK2012823).

REFERENCES

(1) Davis, M. E.; Saldarriaga, C.; Montes, C.; Garces, J. M.; Crowder, C. *Nature* **1988**, *331*, 698.

(2) (a) Dessau, R. M.; Schlenker, J. G.; Higgins, J. B. *Zeolites* **1990**, *10*, 522. (b) Vogt, E. T. L.; Richardson, J. N. *J. Solid State Chem.* **1990**, *87*, 469. (c) Wagner, P.; Yoshikawa, M.; Lovallo, M.; Tsuji, K.; Tsapatsis, M.; Davis, M. E. *Chem. Commun.* **1997**, 2179. (d) Freyhardt, C. C.; Tsapatsis, M.; Lobo, R. F.; Balkus, K. J.; Davis, M. E. *Nature* **1996**, *381*, 295.

(3) (a) Estermann, M.; Mccusker, L. B.; Baerlocher, C.; Merrouche, A.; Kessler, H. *Nature* **1991**, *352*, 320. (b) Hu, Q.; Xu, R.; Li, S.; Ma, Z.; Thomas, J. M.; Jones, R. H.; Chippindale, A. M. *J. Chem. Soc., Chem. Commun.* **1992**, 875.

(4) (a) Zhu, J.; Bu, X.; Feng, P.; Stucky, G. D. *J. Am. Chem. Soc.* **2000**, *122*, 11563. (b) Yang, G.; Sevov, S. C. *J. Am. Chem. Soc.* **1999**, *121*, 8389. (c) Lin, C. H.; Wang, S. L.; Lii, K. H. *J. Am. Chem. Soc.* **2001**, *123*, 4649. (d) Zhou, Y.; Zhu, H.; Chen, Z.; Chen, M.; Xu, Y.; Zhang, H.; Zhao, D. *Angew. Chem., Int. Ed.* **2001**, *40*, 2166. (e) Plevert, J.; Gentz, T. M.; Laine, A.; Li, H. L.; Young, V. G.; Yaghi, O. M.; O'Keeffe, M. *J. Am. Chem. Soc.* **2001**, *123*, 12706. (f) Guillou, N.; Gao, Q.; Nogues, M.; Morris, R. E.; Hervieu, M.; Ferey, G.; Cheetham, A. K. *C. R. Acad. Sci., Ser. IIC* **1999**, *2*, 387. (g) Guillou, N.; Gao, Q.; Forster, P. M.; Chang, J.; Nogues, M.; Park, S. E.; Ferey, G.; Cheetham, A. K. *Angew. Chem., Int. Ed.* **2001**, *40*, 28313. (h) Lin, Z.; Zhang, J.; Zhao, J.; Zheng, S.; Pan, C.; Wang, G.; Yang, G. *Angew. Chem., Int. Ed.* **2005**, *44*, 6881. (i) Liang, J.; Li, J.; Yu, J.; Chen, P.; Fang, Q.; Sun, F.; Xu, R. *Angew. Chem., Int. Ed.* **2006**, *45*, 2546.

(5) Zou, X.; Conradsson, T.; Klingstedt, M.; Dadachov, M. S.; O'Keeffe, M. *Nature* **2005**, *437*, 716.

(6) (a) Rao, C. N. R.; Behera, J. N.; Dan, M. *Chem. Soc. Rev.* **2006**, *35*, 375. (b) Dan, M.; Behera, J. N.; Rao, C. N. R. *J. Mater. Chem.* **2004**, *14*, 1257.

(7) Doran, M. B.; Norquist, A. J.; O'Hare, D. *Chem. Commun.* **2002**, 2946.

(8) (a) Bataille, T.; Louer, D. *J. Mater. Chem.* **2002**, *12*, 3487. (b) Bataille, T.; Louer, D. *J. Solid State Chem.* **2004**, *177*, 1235. (c) Xing, Y.; Liu, Y.; Shi, Z.; Meng, H.; Pang, W. *J. Solid State Chem.* **2003**, *174*, 381. (d) Xing, Y.; Shi, Z.; Li, G.; Pang, W. *Dalton Trans.* **2003**, 940.

(9) Yotnoi, B.; Rujjwatra, A.; Reddy, M. L. P.; Sarma, D.; Narayanan, S. *Cryst. Growth Des.* **2011**, *11*, 1347.

(10) (a) Zhu, Y.; Zhou, G. P.; Xu, Y.; Zhu, D.; Zheng, X. *Z. Anorg. Allg. Chem.* **2008**, *634*, 545. (b) Zhou, W.; Chen, Q.; Zhu, D.; Xu, Y. *Z. Anorg. Allg. Chem.* **2009**, *635*, 572. (c) Zhu, Y.; Sun, X.; Zhu, D.; Xu, Y. *Inorg. Chim. Acta* **2009**, *362*, 2565. (d) Zhou, W.; Chen, Q.; Jiang, N.; Meng, X.; Zhu, D.; Xu, Y. *Inorg. Chim. Acta* **2009**, *362*, 3299. (e) Zhou, W.; Xu, Y.; Han, L.; Zhu, D. *Dalton Trans.* **2010**, 3681. (f) Zhou, W.; Ding, X.; Zhang, Z.; Zheng, L.; Xu, Y.; Zhu, D. *Z. Anorg. Allg. Chem.* **2010**, *636*, 882.

(11) (a) Zheng, L.; Xu, Y.; Zhang, X.; Zhang, Z.; Zhu, D.; Chen, S.; Elangovan, S. P. *CrystEngComm* **2010**, *12*, 694. (b) Zheng, L.; Qiu, X.; Zhang, Z.; Zhu, D.; Xu, Y. *Inorg. Chem. Commun.* **2011**, *14*, 906. (c) Zhang, D.; Zheng, L.; Qiu, X.; Xu, Y.; Fu, J.; Zhu, D. *RSC Adv.* **2012**, *2*, 217. (d) Zheng, L.; Qiu, X.; Xu, Y.; Fu, J.; Yuan, Y.; Zhu, D.;

Chen, S. *CrystEngComm* **2011**, *13*, 2714. (e) Zheng, L.; Zhang, Z.; Zhu, D.; Xu, Y. *Inorg. Chem. Commun.* **2011**, *14*, 258. (f) Ju, W.; Zhang, D.; Zhu, D.; Xu, Y. *Inorg. Chem.* **2012**, *51*, 13373. (g) Zhang, D.; Lu, Y.; Chen, L.; Cai, H.; Zhu, D.; Xu, Y. *CrystEngComm* **2012**, *14*, 6627.

(12) Natarajan, S.; Mandal, S. *Angew. Chem., Int. Ed.* **2008**, *47*, 4798.

(13) (a) Schoedel, A.; Wojtas, L.; Kelley, S. P.; Rogers, R. D.; Eddaoudi, M.; Zaworotko, M. J. *Angew. Chem., Int. Ed.* **2011**, *50*, 11421. (b) Carlucci, L.; Ciani, G.; Maggini, S.; Proserpio, D. M.; Visconti, M. *Chem.—Eur. J.* **2010**, *16*, 12328.

(14) (a) Sudik, A. C.; Cote, A. P.; Yaghi, O. M. *Inorg. Chem.* **2005**, *44*, 2998. (b) Gedrich, K.; Senkovska, I.; Baburin, I. A.; Mueller, U.; Trapp, O.; Kaskel, S. *Inorg. Chem.* **2010**, *49*, 4440. (c) Jeong, S.; Song, X.; Jeong, S.; Oh, M.; Liu, X.; Kim, D.; Moon, D.; Lah, M. S. *Inorg. Chem.* **2011**, *50*, 12133.

(15) (a) Zhang, J.; Meng, S.; Song, Y.; Zhou, Y.; Cao, Y.; Li, J.; Zhao, H.; Hu, J.; Wu, J.; Humphrey, M. G.; Zhang, C. *Cryst. Growth Des.* **2011**, *11*, 100. (b) Lincke, J.; Lassig, D.; Stein, K.; Moellmer, J.; Kuttathayil, A. V.; Reichenbach, C.; Moeller, A.; Staudt, R.; Kalies, G.; Bertmer, M.; Krautscheid, H. *Dalton Trans.* **2012**, *41*, 817. (c) Qiu, Y.; Li, Y.; Peng, G.; Cai, J.; Jin, L.; Ma, L.; Deng, H.; Zeller, M.; Batten, S. R. *Cryst. Growth Des.* **2010**, *10*, 1332. (d) Zhong, D.; Lu, W.; Jiang, L.; Feng, X.; Lu, T. *Cryst. Growth Des.* **2010**, *10*, 739.

(16) (a) Chen, X. A.; Xue, H. P.; Chang, X. A.; Zang, H. G.; Xiao, W. Q. *J. Alloys Compd.* **2005**, *398*, 173. (b) Galez, C.; Mugnier, Y.; Bouillot, J.; Lambert, Y.; Le Dantec, R. *J. Alloys Compd.* **2006**, *416*, 261. (c) Phanon, D.; Mosset, A.; Gautier-Luneau, I. *J. Mater. Chem.* **2007**, *17*, 1123. (d) O'Keeffe, M.; Peskov, M. A.; Ramsden, S. J.; Yaghi, O. M. *Acc. Chem. Res.* **2008**, *41*, 1782.

(17) Zhao, D. Y.; Feng, J. L.; Huo, Q. S.; Melosh, N.; Fredrickson, G. H.; Chmelka, B. F.; Stucky, G. D. *Science* **1998**, *279*, 548.

(18) Sheldrick, G. M. *SHELXTL*, version 5.10; Bruker AXS Inc.: Madison, WI, 1997.

(19) (a) Bataille, T.; Louer, D. *J. Mater. Chem.* **2002**, *12*, 3487. (b) Jayaraman, K.; Choudhury, A.; Rao, C. N. R. *Solid State Sci.* **2002**, *4*, 413.